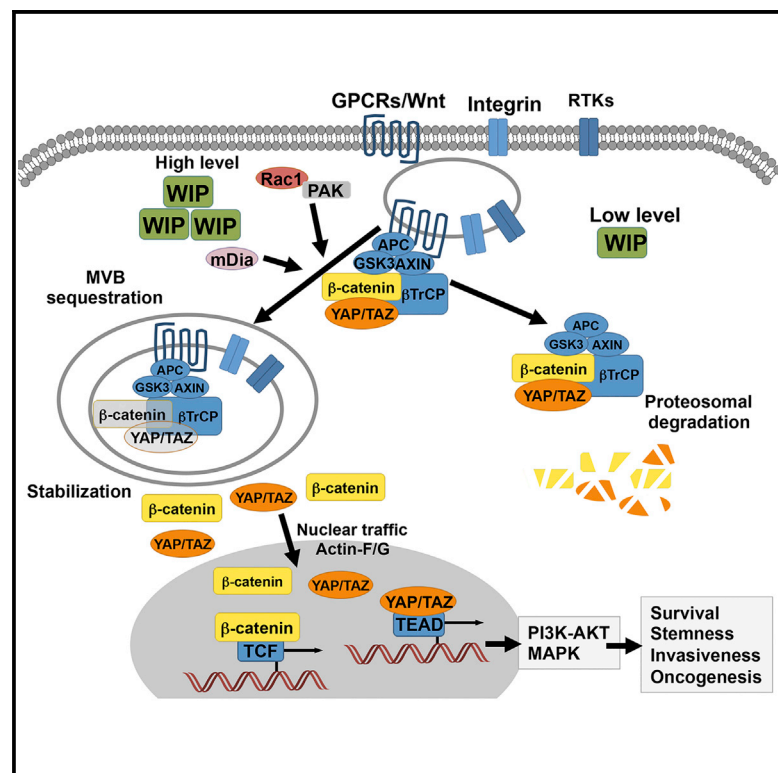


## WIP Drives Tumor Progression through YAP/TAZ-Dependent Autonomous Cell Growth

### Graphical Abstract



### Authors

Ricardo Gargini, Maribel Escoll,  
Esther García, Ramón García-Escudero,  
Francisco Wandosell, Inés María Antón

### Correspondence

fwandosell@cbm.csic.es (F.W.),  
ianton@cnb.csic.es (I.M.A.)

### In Brief

Gargini et al. show that WIP stabilizes the transcriptional co-activators YAP/TAZ via the endocytic/endosomal system, suggesting that WIP has oncogenic functions. WIP promotes and coordinates cell proliferation, stemness, and invasiveness to drive tumor progression.

### Highlights

- High WIP levels promote YAP/TAZ stability and correlate with poor patient survival
- WIP regulates the endocytic/endosomal system via Rac/PAK and the formin mDia
- WIP expression leads to sequestration of the  $\beta$ -catenin destruction complex in MVB
- WIP reduction impairs *in vivo* glioblastoma growth, notably increasing mouse survival

# WIP Drives Tumor Progression through YAP/TAZ-Dependent Autonomous Cell Growth

Ricardo Gargini,<sup>1,2,3,6</sup> Maribel Escoll,<sup>2,3,6</sup> Esther García,<sup>1,3</sup> Ramón García-Escudero,<sup>4,5</sup> Francisco Wandosell,<sup>2,3,\*</sup> and Inés María Antón<sup>1,3,7,\*</sup>

<sup>1</sup>Centro Nacional de Biotecnología (CNB-CSIC), Darwin 3, 28049 Madrid, Spain

<sup>2</sup>Centro de Biología Molecular Severo Ochoa (CSIC-UAM), Nicolás Cabrera 1, Universidad Autónoma de Madrid, 28049 Madrid, Spain

<sup>3</sup>Centro de Investigación Biomédica en Red de Enfermedades Neurodegenerativas (CIBERNED), 28031 Madrid, Spain

<sup>4</sup>Molecular Oncology Unit, CIEMAT (ed70A), 28040 Madrid, Spain

<sup>5</sup>Biomedical Research Institute I+12, University Hospital 12 de Octubre, 28041 Madrid, Spain

<sup>6</sup>Co-first author

<sup>7</sup>Lead Contact

\*Correspondence: [fwandosell@cbm.csic.es](mailto:fwandosell@cbm.csic.es) (F.W.), [ianton@cnb.csic.es](mailto:ianton@cnb.csic.es) (I.M.A.)

<http://dx.doi.org/10.1016/j.celrep.2016.10.064>

## SUMMARY

In cancer, the deregulation of growth signaling pathways drives changes in the cell's architecture and its environment that allow autonomous growth of tumors. These cells then acquire a tumor-initiating "stemness" phenotype responsible for disease advancement to more aggressive stages. Here, we show that high levels of the actin cytoskeleton-associated protein WIP (WASP-interacting protein) correlates with tumor growth, both of which are linked to the tumor-initiating cell phenotype. We find that WIP controls tumor growth by boosting signals that stabilize the YAP/TAZ complex via a mechanism mediated by the endocytic/endosomal system. When WIP levels are high, the  $\beta$ -catenin Adenomatous polyposis coli (APC)-axin-GSK3 destruction complex is sequestered to the multi-vesicular body compartment, where its capacity to degrade YAP/TAZ is inhibited. YAP/TAZ stability is dependent on Rac, p21-activated kinase (PAK) and mammalian diaphanous-related formin (mDia), and is Hippo independent. This close biochemical relationship indicates an oncogenic role for WIP in the physiology of cancer pathology by increasing YAP/TAZ stability.

## INTRODUCTION

A common feature of many tumors is their dependence on survival signals such as upregulation of the phosphatidylinositol 3-kinase (PI3K)-AKT and mitogen-activated protein kinase (MAPK) pathways (Hanahan and Weinberg, 2011), which allow some autocrine signaling. Many tumor cell types nonetheless depend on endo- or exocytosis for their growth, migration, and invasion (Joffre et al., 2011). It was initially considered that the only role of endocytosis was to restrict signals by internaliza-

tion of membrane receptors, but it was later shown that the endosomal system also has a central role as a second round of signals that determine the final effect of these receptors (Dobrowolski and De Robertis, 2011). The regulation of actin polymerization is central to coordinating receptor-mediated endocytosis as well as receptor recycling and degradation (Schafer, 2002). Some of these processes also require actin cytoskeleton dynamics to coordinate cell proliferation and invasion, which are associated with metastasis. Several regulatory and actin-associated molecules, such as WASP (Wiskott-Aldrich syndrome protein) family proteins or WIP (WASP-interacting protein) participate in migration and invadopodium formation, which might sustain metastasis (Stevenson et al., 2012), but only a few have essential roles in cancer pathology.

The YAP/TAZ complex of transcriptional co-activators is directly implicated in tumor development and cancer stem cell or tumor-initiating cells (TICs) (Cordenonsi et al., 2011). The  $\beta$ -catenin destruction complex (adenomatous polyposis coli [APC]/axin/GSK3), which controls  $\beta$ -catenin transcriptional activity in the Wnt pathway, regulates YAP/TAZ stability and transcription (Azzolin et al., 2012, 2014). YAP/TAZ binds axin, which allows the complex to interact with its ubiquitin ligase  $\beta$ TrCP, which facilitates ubiquitination and subsequent degradation of YAP/TAZ and  $\beta$ -catenin (Azzolin et al., 2012, 2014). This mechanism coordinates the regulation of these transcription factors. APC/axin/GSK3 can be sequestered in the multivesicular bodies (MVBs) of the endosomal compartment, which blocks  $\beta$ -catenin degradation, a key step in Wnt signaling induction. Formation of the degradation complex and its sequestration could amplify Wnt signaling for  $\beta$ -catenin (Taelman et al., 2010).

Here we show the involvement of the actin regulator WIP in cancer progression. We describe a pro-tumor relationship between WIP levels and those of the transcriptional co-activators YAP/TAZ. WIP also mediates cell growth signals such as MAPK, a function controlled by the endocytic/endosomal systems, which sequester the APC/axin/GSK3 degradation complex and promote YAP/TAZ stability. This WIP-mediated YAP/TAZ stability is supported by a close correlation in the expression of these proteins. Moreover, we show that WIP controls YAP/TAZ

levels in several in vitro models; it acts as a master regulator of pro-tumor functions such as proliferation and cell survival and promotes the establishment of stemness and invasiveness. By modifying the endocytic/endosomal systems to block degradation of YAP/TAZ and  $\beta$ -catenin transcription factors, by promoting autocrine growth, by favoring TIC generation, and by allowing establishment of an aggressive tumor phenotype, WIP shows certain characteristics of an oncogene.

## RESULTS

### WIP Correlates with a High Tumor Proliferation Rate and Stemness

Although several studies have implicated the actin cytoskeleton in cancer pathology (Stevenson et al., 2012), actin-associated proteins such as WIP have not been connected specifically to tumor transformation or acquisition of stem phenotypes. We analyzed the expression of WIP and of the proliferative marker Ki67 in brain tissue samples from patients with glioblastoma multiforme (GB) and controls (Figures 1A–1G) as well as WIP expression in tumor cell lines derived from various cancer types (Figure S1A). WIP was significantly overexpressed in GB compared with normal brain tissue ( $p = 3 \times 10^{-7}$ ) (Figure 1A) and, within the GB panel, was increased in the more aggressive mesenchymal subtype (Figure S1B). In tumor cells derived from GB patient surgical specimens, stem marker CD133 levels were high in three explants (GB4, 5, and 8) cultured under stem conditions (which favors the TIC population) and low when grown in DMEM with 10% fetal bovine serum (FBS) (DMEM 10%, Adherent) (Figure 1C). Biochemical analysis indicated differential WIP expression (Figure 1D). Immunofluorescence (IF) analysis of tumor spheres showed a greater proliferative capacity (Ki67<sup>+</sup> cells) of high WIP-expressing GB4 and GB8 compared with low proliferative, low WIP-expressing GB7 and GB11 (Figures 1B and 1E–1G). Two WIP-specific small hairpin RNAs (shRNAs) significantly impaired cell growth under stem conditions, followed by 4,5-dimethylthiazol-2-yl (MTT) assay (Figures S1C–S1F), or as secondary spheres, or under anchorage-independent (soft agar) growth conditions (Figures 1H–1K).

Western blot analysis from fluorescence-activated cell sorting (FACS)-purified CD44<sup>Low</sup>/CD24<sup>High</sup> cell and CD44<sup>High</sup>/CD24<sup>Low</sup> (TIC) populations indicated that WIP expression was increased in TICs (Figure S1G). In parallel, we used extreme limiting dilution analysis to assay cell capacity to generate tumor spheres. CD44<sup>High</sup>/CD24<sup>Low</sup> TIC population growth was severely impeded by WIP knockdown (Figure S1H). These data show a direct relationship between high tumor proliferation and stemness levels and high WIP levels in patient-derived samples.

### WIP Levels Correlate with YAP/TAZ and Are Crucial for Tumor Progression In Vitro and In Vivo

YAP/TAZ levels are specifically increased in several human cancers and are fundamental for maintenance, proliferation, and tumor initiation in breast cancer stem cells (Moroishi et al., 2015). Western blot analysis of a panel of human brain tissue samples, using an antibody that recognizes both proteins, showed significant correlation between WIP and YAP or TAZ levels (Figures 2A and 2B). We tested additional cell lines of other

cancer lineages and again observed a close correlation between WIP and YAP or TAZ levels (Figures S2A and S2B). To determine whether there is direct WIP and YAP/TAZ interdependence, we knocked down WIP in two GBs (U373-MG and GB4), which acutely reduced YAP/TAZ expression to levels of untransformed control human astrocytes and impaired cell growth in soft agar (Figures 2C and 2D). The results were similar in a breast carcinoma model in which high WIP levels correlated with high YAP/TAZ expression in mesenchymal phenotypes; WIP reduction decreased the TIC population (CD44<sup>High</sup>/CD24<sup>Low</sup>) (Figures S2C and S2D).

To test for underlying molecular connections, we knocked down WIP, YAP, or TAZ in GB4, GB5, and GB8 cells and analyzed growth. WIP knockdown reduced YAP and TAZ levels (Figure 2E), and knockdown of WIP, TAZ, or YAP decreased tumor sphere growth and cell number (Figures 2F and 2G; data not shown) and induced apoptosis in all three GBs (Figure 2H; data not shown). In a confirmatory cell culture system, we verified that WIP reduction affected both YAP/TAZ levels and nuclear localization (Figure S2E). To determine whether interference with WIP expression had a similar inhibitory effect in vivo to that observed in vitro, we transduced GB cells with shRNA against WIP or a non-target control and injected the cells stereotactically into the non-obese diabetic/severe combined immunodeficiency (NOD/SCID) mouse striatum. WIP elimination impaired tumor growth and caused a notable increase in mouse survival (Figures 2I–2K). This WIP reduction effect was confirmed in patient samples. As shown by Kaplan-Meier analyses in two datasets for human GB, tumors with low or intermediate WIP levels correlated with a significantly greater probability of increased patient survival compared with tumors characterized by high WIP expression (Figures 2L and 2M). To determine whether this correlative expression of WIP and YAP/TAZ is restricted to solid tumors, we analyzed hematological cancers with high WIP levels and YAP/TAZ-independent growth (Figures S2F–S2H; Cottini et al., 2014). In these models, in which YAP/TAZ is not expressed, WIP elimination had no effect on tumor growth (Figures S2I–S2K).

These data support an essential role for WIP in maintaining YAP/TAZ-dependent TIC growth and phenotype, which is imperative for in vivo solid tumor growth.

### High WIP Levels Upregulate YAP/TAZ Expression and Promote Tumor Growth and Stemness

We analyzed whether WIP overexpression affected the growth of normal human cells. Lentiviral expression of WIP-GFP in primary human astrocytes increased YAP/TAZ expression, enhanced proliferative signals such as phospho extracellular signal-regulated kinase (pERK), and potentiated the YAP/TAZ targets connective tissue growth factor (CTGF) and caveolin; these signals triggered tumor sphere formation and cell growth (Figures 3A–3C; Figures S3A and S3B). This WIP-GFP effect was similar in normal MCF10A breast cells (data not shown). In the WIP-overexpressing model, shRNA interference of WIP, YAP, or TAZ greatly reduced growth capacity and proliferative marker expression and triggered apoptosis (Figures 3A–3D).

WIP has several interaction regions: the WASP/neural Wiskott Aldrich Syndrome protein (N-WASP)-binding domain,

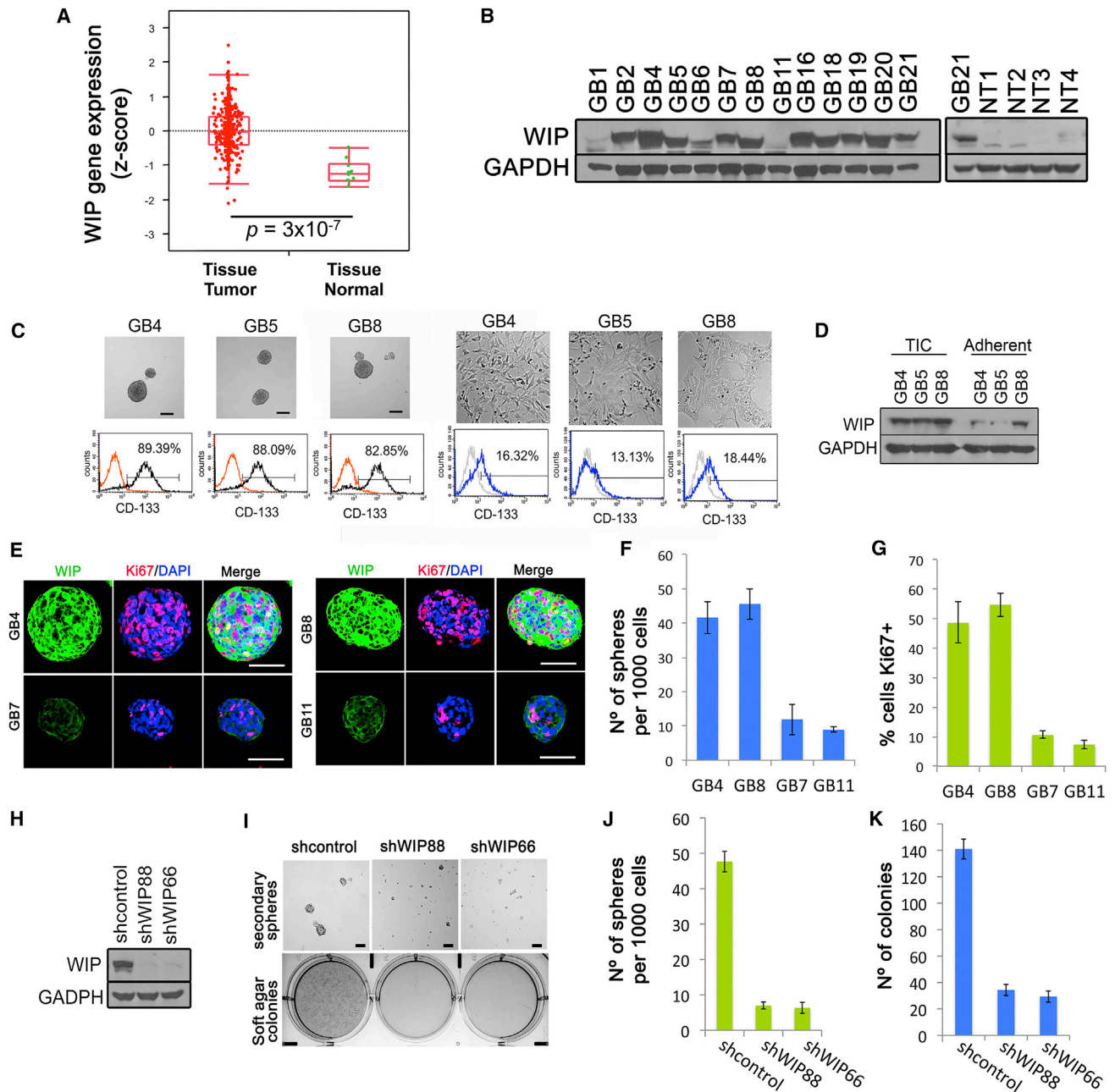


**Figure 1. WIP Expression Correlates with Tumor Growth and Is Associated with the TIC Phenotype**

(A) WIP mRNA is overexpressed in GB tumors compared with normal brain. Significant differences were calculated using Student's t test.  
 (B) Western blot analysis of WIP and glyceraldehyde-3-phosphate dehydrogenase (GAPDH) as a control in a panel of extracts from human GB tumor tissue compared with normal tissue (NT).  
 (C) Left: representative images of GB4, GB5, and GB8 cultured under stem conditions and showing high CD133 expression. Right: equivalent analysis of adherent cultures in DMEM-10% FBS. Scale bars, 50  $\mu$ m.  
 (D) Western blot analysis of WIP and GAPDH expression.  
 (E–G) Tumor sphere-forming ability of explants from GB patients.  
 (E) Representative confocal image of WIP and Ki67 expression and DAPI nuclear staining in tumor spheres from GB4 and GB8 (high WIP expression) and GB7 and GB11 (low WIP expression). Scale bars, 50  $\mu$ m.  
 (F and G) Number of spheres formed (F) and percentage of Ki67<sup>+</sup> cells (G).  
 (H) Western blot analysis of WIP and GAPDH in MDA-MB-231 cells transduced with two specific lentiviral shRNAs against WIP.  
 (I) Representative images of growth under stem conditions (top; scale bars, 50  $\mu$ m) and anchorage-independent growth conditions (soft agar, bottom).  
 (J and K) Number of spheres formed (J) and colony number in soft agar (K).  
 (F, G, J, and K) Data are shown as mean  $\pm$  SEM (n = 3).

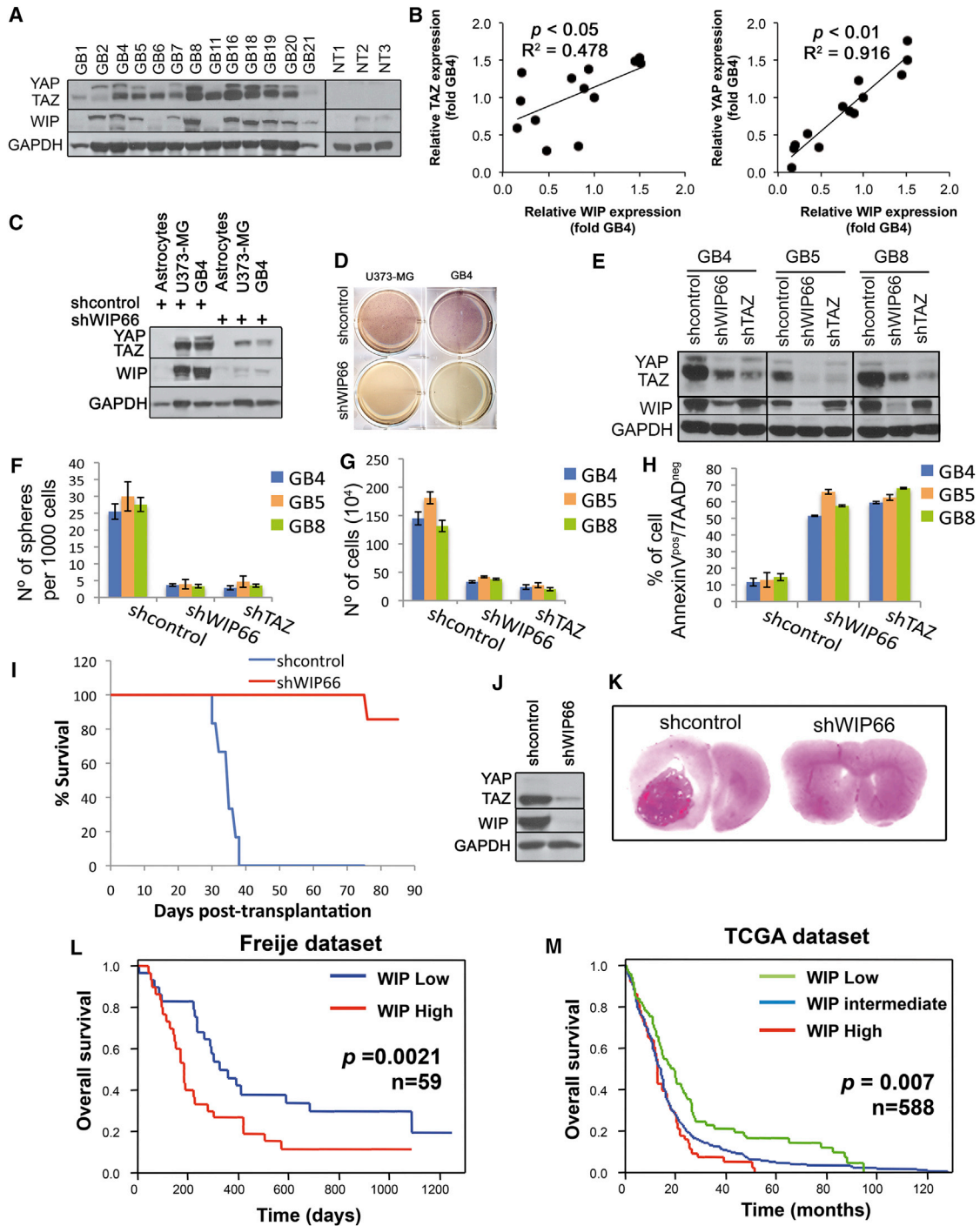


**Figure 2. WIP Requirement for In Vitro and In Vivo Tumor Growth Is YAP/TAZ-Dependent**

(A) Western blot analysis of YAP/TAZ, WIP, and GAPDH control in a panel of extracts from human GB tumor tissue compared with NT.

(B) Quantification of the correlation between YAP or TAZ versus WIP expression shown in (A).

(C) Western blot analysis of WIP and YAP/TAZ in extracts from astrocytes and from U373-MG and GB4 explant cells transduced with control shRNA (shcontrol) or against WIP (shWIP66), all cultured under stem conditions.

(D) Representative images of shcontrol- or shWIP66-transduced U373-MG and GB4 explant cells grown in soft agar (7 days).

(E) Western blot analysis of YAP/TAZ, WIP, and GAPDH in GB4, GB5, and GB8 samples knocked down for WIP, TAZ, or control.

(F–H) Quantification of the number of spheres (F), cells (trypan blue exclusion) (G), and cell death (annexin V/7-aminocoumarinyl fluorescein [7-AAD]) by flow cytometry (H) generated by WIP, TAZ, or control knockdown as in (E). Data are shown as mean  $\pm$  SEM ( $n = 3$ ).

(legend continued on next page)

the actin-binding domain, and a proline-rich region that binds cortactin, profilin, the actin-binding protein (Abp-1), as well as the adaptors Nck and CrkL (Antón et al., 2007). To determine whether the complete protein is necessary for WIP transformation capacity, we transduced human astrocytes with lentiviruses that encode three WIP constructs: full-length, WIP- $\Delta$ NBD (lacking the Nck-binding domain), or WIP- $\Delta$ 42-53 (lacking the actin-binding domain) (Figure 3E; García et al., 2012). Determination of tumor sphere number and CD133 levels showed that only the full-length version enhanced cell growth and stemness (Figures 3E–3G; Figures S3C and S3D).

### WIP Regulates Cell Invasion in a YAP/TAZ-Dependent Manner

Two striking features of TICs are their plasticity and their enhanced metastatic potential. We therefore used highly metastatic MDA-MB-231 cells (Muller et al., 2009) to test whether WIP regulates their invasiveness. MDA-MB-231 cells have a large proportion of TICs, as shown by the number of invasive Matrigel-3D structures, which have high nuclear YAP/TAZ levels (Figures 4A and 4B). Elimination of WIP in these cells suppressed formation of these invasive structures nearly completely and appeared to impair growth (Figures 4A and 4B). In a complementary approach, we tested whether WIP overexpression stimulates these features in the low metastatic MDA-MB-468 cell line. We used GFP-, WIP-GFP-, WIP- $\Delta$ NBD-, and WIP- $\Delta$ 42-53-encoding lentiviruses. As seen in primary astrocytes, only full-length WIP increased TAZ levels and stemness in MDA-MB-468 cells (Figures 4C–4E). In addition, overexpression of full-length WIP greatly increased MDA-MB-468 cell invasiveness (Figures 4F and 4G).

To link this WIP function with YAP/TAZ, we knocked down WIP, YAP, or TAZ in WIP-overexpressing breast tumor cells; elimination of any of these proteins reestablished their naturally low cell invasiveness (Figures 4H and 4I). The effects generated by WIP overexpression, including increased proliferation, survival, stemness, and invasiveness, might thus be coordinated. We confirmed that WIP increased cell proliferation and promoted YAP/TAZ nuclear transit specifically in invasive structures, which corroborated coordination of these processes (Figures S4A–S4C). In parallel, WIP overexpression suppressed the spontaneous basal cell death that normally occurs in the fraction of non-invasive structures (Figures S4D and S4E). These proliferative processes are linked to increased invasiveness, essential for metastasis generation (Shibue et al., 2013), as confirmed by our findings.

### WIP Controls YAP/TAZ Stability Independently of the Hippo Pathway and Actin Polymerization

Our results strongly suggested that WIP expression upregulates YAP/TAZ, whereas its downregulation decreases YAP/TAZ. To

analyze the mechanism that underlies this regulation, we tested whether WIP modifies YAP/TAZ mRNA expression in WIP shRNA-transduced GB4, GB5, and GB8 cells. qRT-PCR data showed no notable differences in TAZ mRNA levels in these cells (Figure S5A). Because YAP/TAZ is degraded by the proteasome (Liu et al., 2010), we tested whether WIP uses this system to degrade YAP/TAZ. WIP knockdown GB4, GB5, and GB8 cells treated with the proteasome inhibitor MG132 showed significant recovery of YAP/TAZ levels (Figures 5A and 5B). We thus speculated that WIP controls the proteasome-mediated degradation system. Using a degradation-insensitive TAZ mutant (TAZ-S311A) (Liu et al., 2010), we observed recovery of all processes otherwise affected by WIP elimination, including proliferation, stemness, and invasiveness (Figures 5C–5I; Figure S5B). This mutant also rescued the decrease in TEA domain (TEAD)- and  $\beta$ -catenin-dependent transcription produced by WIP reduction (Figures S5C and S5D).

In the Hippo system, an Mst1/2- and Lats1/2-mediated kinase cascade phosphorylates YAP/TAZ, tagging this complex for proteasome degradation. Actin controls YAP/TAZ stability and nuclear localization, although the mechanism is not fully understood (Piccolo et al., 2014). Although the Hippo pathway has been established as the main link between actin polymerization and YAP/TAZ transcriptional activity (Aragona et al., 2013; Dupont et al., 2011), an alternative Hippo-independent mechanism could explain YAP/TAZ regulation by actin polymerization in some other cancer-related models (Dupont et al., 2011; Feng et al., 2014). To define the mechanism by which WIP regulates YAP/TAZ levels, we analyzed whether actin polymerization or depolymerization affect YAP/TAZ stability in the absence of WIP. MDA-MB-231 cells transduced with shRNAs to WIP or a control were incubated with latrunculin A1 (Lata1), a filamentous actin (F-actin)-depolymerizing agent, or jasplakinolide, an F-actin stabilizer. Neither treatment re-established YAP/TAZ levels after degradation by WIP knockdown (Figure 5J) or affected YAP/TAZ nuclear transit (Figure 5K).

We also tested whether increased Hippo activity modifies WIP-mediated YAP/TAZ stability. Human GFP- or GFP-WIP-expressing astrocytes were transduced with lentiviruses encoding Lats1, Mst2, or both. Despite increased YAP phosphorylation, WIP-GFP-expressing astrocytes maintained YAP/TAZ stability and sphere-forming capacity under stem culture conditions when the Hippo pathway was hyperactivated by Mst2/Lats1 (Hao et al., 2008; Figures S5E and S5F). In a complementary experiment, we observed that, in the absence of WIP, Lats1/2 elimination did not rescue YAP/TAZ stability or cell growth (Figures S5G and S5H). Finally, we used a mutant version of YAP (S5A) in which all Lats1 phosphorylation sites are mutated to alanine to generate a stable, active protein. Astrocytes were infected with YAP wild-type (WT) or YAP-S5A lentivirus and then

(I) Kaplan-Meier survival curves of mice orthotopically implanted in the brain with GB cells transduced with a lentivirus encoding shcontrol or shWIP (n = 6). Log-rank test;  $p < 10^{-4}$ .

(J) Western blot analysis of WIP, YAP/TAZ, and GAPDH control.

(K) Representative images of brain with H&E staining of the experiment described in (I).

(L) Survival curves in the Freije dataset. Patients were stratified in two equal groups using the median WIP expression value as the cutoff point.

(M) Survival curves in the TCGA GB dataset. Patients were stratified in three groups using WIP Z score values. Significance differences in survival between groups were calculated using the log rank-test.

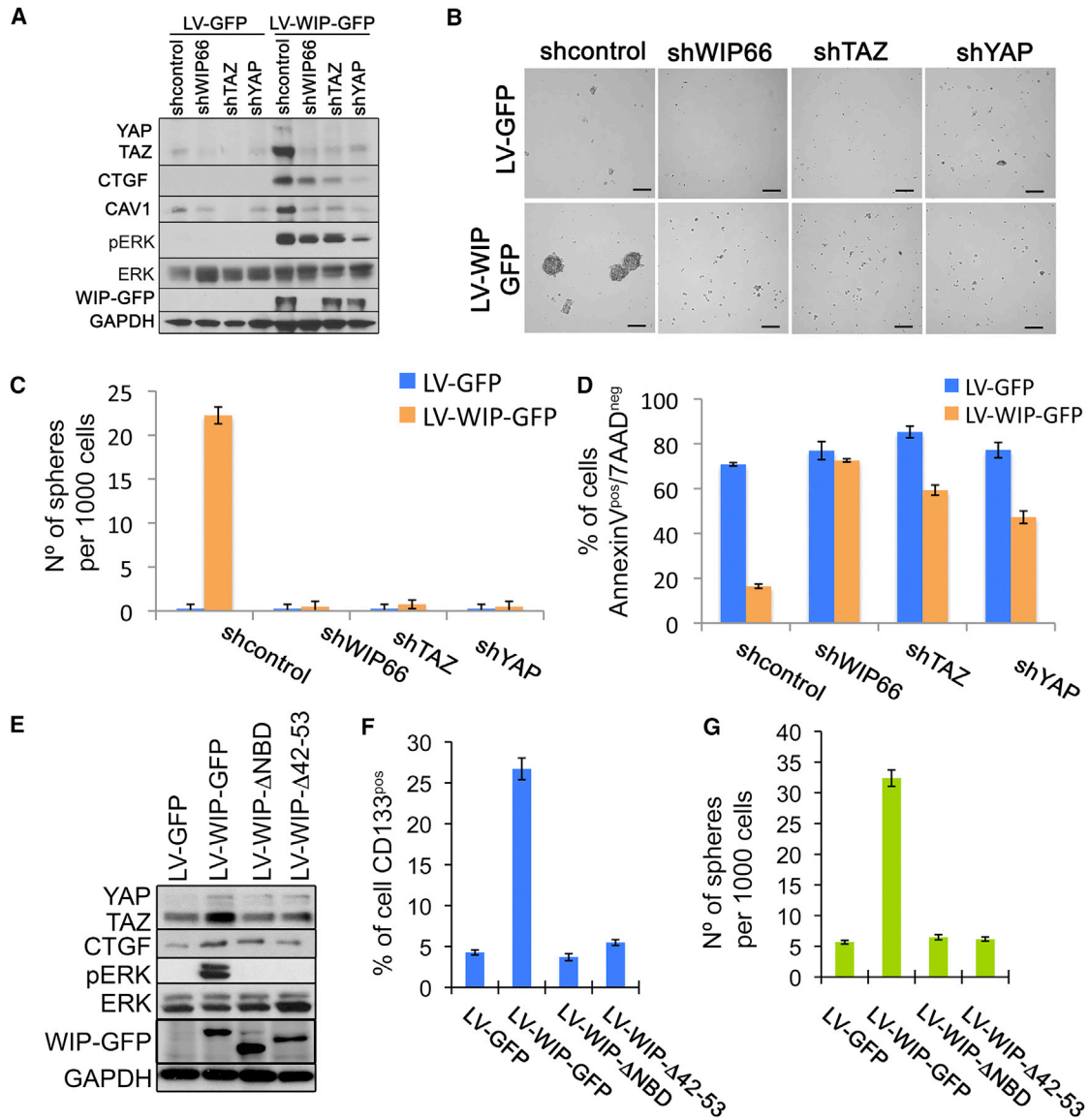


**Figure 3. Overexpression of Full-Length WIP Increases Proliferation, and WIP Is Necessary to Establish the Epithelial-Mesenchymal Transition by the Control Exercised over YAP/TAZ**

(A–D) Astrocytes expressing GFP or WIP-GFP and transduced with a lentivirus encoding WIP-, TAZ-, YAP-, or control-specific shRNA were cultured as tumor spheres (stem conditions, 6 days).

(A) Western blot analysis of YAP/TAZ, CTGF, CAV1, pERK, ERK, WIP-GFP, and GAPDH levels.

(B) Representative image of sphere growth. Scale bars, 50  $\mu$ m.

(C and D) Quantification of sphere number (C) and cell death (D) measured by annexin V/TAAD staining.

(E–G) Astrocytes were transduced with a lentivirus encoding GFP, full-length WIP (WIP-GFP), WIP lacking the Nck binding site (WIP- $\Delta$ NCK), or the actin binding site (WIP- $\Delta$ 42-53).

(E) Western blot analysis of YAP/TAZ, CTGF, pERK, ERK, WIP-GFP, and GAPDH expression.

(F) Percentage of CD133<sup>+</sup> cells by flow cytometry.

(G) Number of spheres.

(C, D, F, and G) Data are shown as mean  $\pm$  SEM (n = 3).

transduced with shRNAs against WIP, TAZ, or a non-target control. YAP-S5A increased growth and sphere generation by control cells, whereas WIP or TAZ elimination severely impeded this effect (Figures S5I and S5J), suggesting that the YAP/TAZ

level does not depend on the Hippo pathway-mediated phosphorylation in cells with a reduced WIP level. All of our western blot data suggest that YAP and TAZ cooperate to form a complex essential for stemness (Figures 2E and 3A; Figures S3A

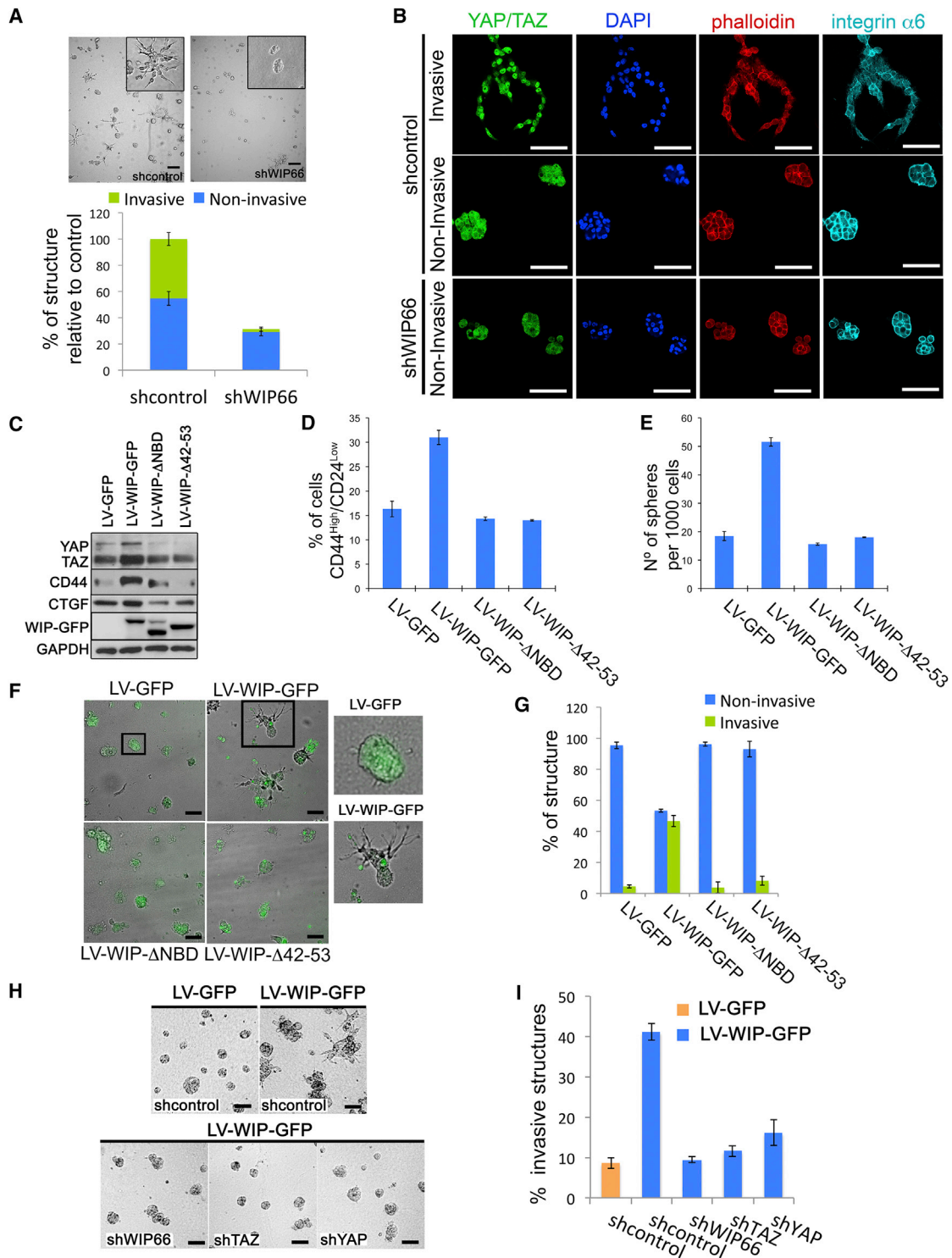


**Figure 4. WIP Increases Cell Survival and Proliferation by Promoting the TIC Phenotype and Drives YAP/TAZ-Dependent Cell Invasion**  
 (A) Top: representative images of Matrigel-seeded MDA-MB-231 cells knocked down for WIP or control. Scale bars, 25  $\mu$ m. Bottom: percentage of invasive and non-invasive structures (at least 100 individual structures in each of three independent experiments, relative to shcontrol).  
 (B) Confocal images of the staining for YAP/TAZ (green), nuclei (DAPI, blue), F-actin (phalloidin, red), and integrin  $\alpha$ 6 (cyan) of invasive and non-invasive structures in 3D Matrigel as described in (A). Scale bars, 25  $\mu$ m.

(legend continued on next page)



and S5I) and that, although they might replace each other partially, there is a minimum threshold of each for activity. These results indicate that the WIP-mediated stability of YAP/TAZ is not compensated by actin stabilization, nor is it sensitive to Hippo activation.

### WIP Regulates the Endocytosis and/or Multivesicular System to Control YAP/TAZ Levels

Cancer cells often bear multiple genetic alterations that complicate the description of oncogenic pathways. To overcome this drawback and to specifically evaluate WIP-transforming capacity, we overexpressed WIP-GFP in normal primary human astrocytes, which have an unmodified genetic background. WIP overexpression reduced cell death of these astrocytes (control WIP-GFP; Figure 6A). To identify the signaling pathways involved, we sought molecules able to reverse WIP-mediated survival. We quantified cell death of primary astrocytes incubated with a panel of inhibitors of different protein activities (kinases, GTPases, actin regulators, and ionophores). Inhibitors of WIP-related proteins had no effect, including inhibitors of N-WASP (wiskostatin, 187-1), Arp2/3 (CK666 and CK869) and Cdc42 (casin) (Figure 6A). In contrast, inhibitors of Rac (NSC23766), p21-activated kinase (PAK; IPA-3), formins (SMIFH2), and the Na<sup>+</sup>/H<sup>+</sup> exchanger (ethyl-isopropyl amiloride [EIPA]) as well as monovalent cation ionophores (monensin, nigericin, and salinomycin) were specifically cytotoxic for WIP-overexpressing astrocytes (red star, Figure 6A). To study the mechanisms involved in WIP-transforming ability, we analyzed EIPA and ionophore capacity to inhibit the endocytic/endosomal system and to specifically kill TICs (Boucrot et al., 2015; Gupta et al., 2009). We validated the effect of these compounds in the GB model, in which they destabilized YAP/TAZ and inhibited cell growth capacity and stemness (Figures S6A and S6B). In MDA-MB-231 cells, WIP elimination prevented endocytosis-mediated transferrin uptake (Figure 6B), and, in these cells and GB4, it disturbed endosomal function, as analyzed by acridine orange staining, cathepsin activity (Magic Red), and endosomal pH (LysoSensor) (Figures S6C–S6E). These results suggest that WIP-transforming ability acts through Rac/PAK/formin activities and affects endosomal function.

### WIP Contributes to $\beta$ -catenin and Wnt Signaling by Sequestering the Degradation Complex in MVBs

Because our data indicated that WIP can regulate endocytosis, and recent reports show that YAP/TAZ is a Wnt signaling target (Azzolin et al., 2012, 2014), we hypothesized that WIP is directly involved in Wnt signaling. We used two strategies to test this hypothesis. We analyzed  $\beta$ -catenin activation and then measured

$\beta$ -catenin-dependent transcription in the TOP/FOP system. WIP elimination reduced levels of active  $\beta$ -catenin (ABC- $\beta$ -catenin) as well as of its cyclin D1 target and of TOP/FOP-dependent transcription (Figures 6C and 6D). Elimination of WIP,  $\beta$ -catenin, or TAZ in MDA-MB-231 cells similarly impaired TIC growth (Figures S6F and S6G), which suggests that all three proteins are common elements of a shared pathway.

To unambiguously establish WIP involvement in Wnt signaling, we tested whether the Wnt3a ligand stabilized YAP/TAZ in WIP-GFP-expressing astrocytes. In ligand-stimulated cells, WIP specifically enhanced YAP/TAZ stability (Figure 6E). Conversely, we tested the effect of WIP reduction in combination with mutant  $\beta$ -catenin and APC, both of which impede  $\beta$ -catenin degradation by the APC/axin/GSK3 destruction complex (Azzolin et al., 2012, 2014). In WIP knockdown cells,  $\beta$ -catenin or APC mutants impeded YAP/TAZ degradation, both when they were overexpressed exogenously (Figure S6H) or when APC was mutated endogenously in colon carcinoma HT29, SW480, and SW620 cells (Figure S6I). In these carcinomas, WIP elimination produced no changes in cell growth (Figure S6J). These findings provide evidence that the  $\beta$ -catenin destruction complex could be WIP-regulated.

A possible link among the various systems affected by WIP was recently reported for Wnt signaling, in which APC/axin/GSK3 is sequestered in MVBs after Wnt ligand stimulation and, thus, prevents  $\beta$ -catenin degradation (Taelman et al., 2010; Vinyoles et al., 2014). To determine whether WIP controls MVB sequestration of the destruction complex, we analyzed WIP localization by immunostaining and found that WIP co-distributed with CD63, a component of MVB intraluminal vesicles (Figure 6F). In addition, a proteinase K protection assay showed that WIP elimination greatly reduced axin and GSK3 levels within MVBs (Figure 6G); this supports a model in which WIP regulates the subcellular distribution of the complex as well as its subsequent degradative activity. In a confirmatory experiment, we analyzed GSK3 and YAP/TAZ subcellular localization in control or WIP knockdown cells and observed that GSK3 co-distributed with LysoTracker staining in cells with high nuclear YAP/TAZ levels; this pattern was severely impaired in the absence of WIP (Figure 6H).

We used two additional approaches to confirm that WIP mediates APC/axin/GSK3 sequestration by MVBs: one using the MVB-specific proteins Rab5 and Hrs and another in which we increased APC/axin/GSK3 sequestration using the lysosome inhibitors bafilomycin and chloroquine. Overexpression of exogenous active Rab5QL and Hrs rescued the YAP/TAZ levels destabilized by WIP knockdown (Figure 6I), whereas neither bafilomycin nor chloroquine rescued YAP/TAZ levels

(C–G) MDA-MB-468 cells transduced with a lentivirus encoding GFP, WIP-GFP, or the deletion mutants WIP- $\Delta$ NBD and WIP- $\Delta$ 42–53, cultured under stem conditions (6 days).

(C) Western blot analysis of cell extracts for YAP/TAZ, CD44, CTGF, WIP-GFP, and GAPDH expression.

(D) Percentage of CD44<sup>High</sup>/CD24<sup>Low</sup> cells by flow cytometry.

(E) Number of spheres formed.

(F and G) Representative image of invasive or non-invasive structure formation in 3D Matrigel (F) (scale bars, 25  $\mu$ m) and quantification of these structures (G).

(H and I) LV-GFP- or LV-WIP-GFP-transduced MDA-MB-468 cells were infected with lentiviral shcontrol, shWIP66, shTAZ, or shYAP. Shown are representative images after 3D Matrigel culture (H, scale bars, 25  $\mu$ m) and the percentage of invasive structures formed (I).

(D, E, G, and I) Data are shown as mean  $\pm$  SEM ( $n \geq 3$ ).

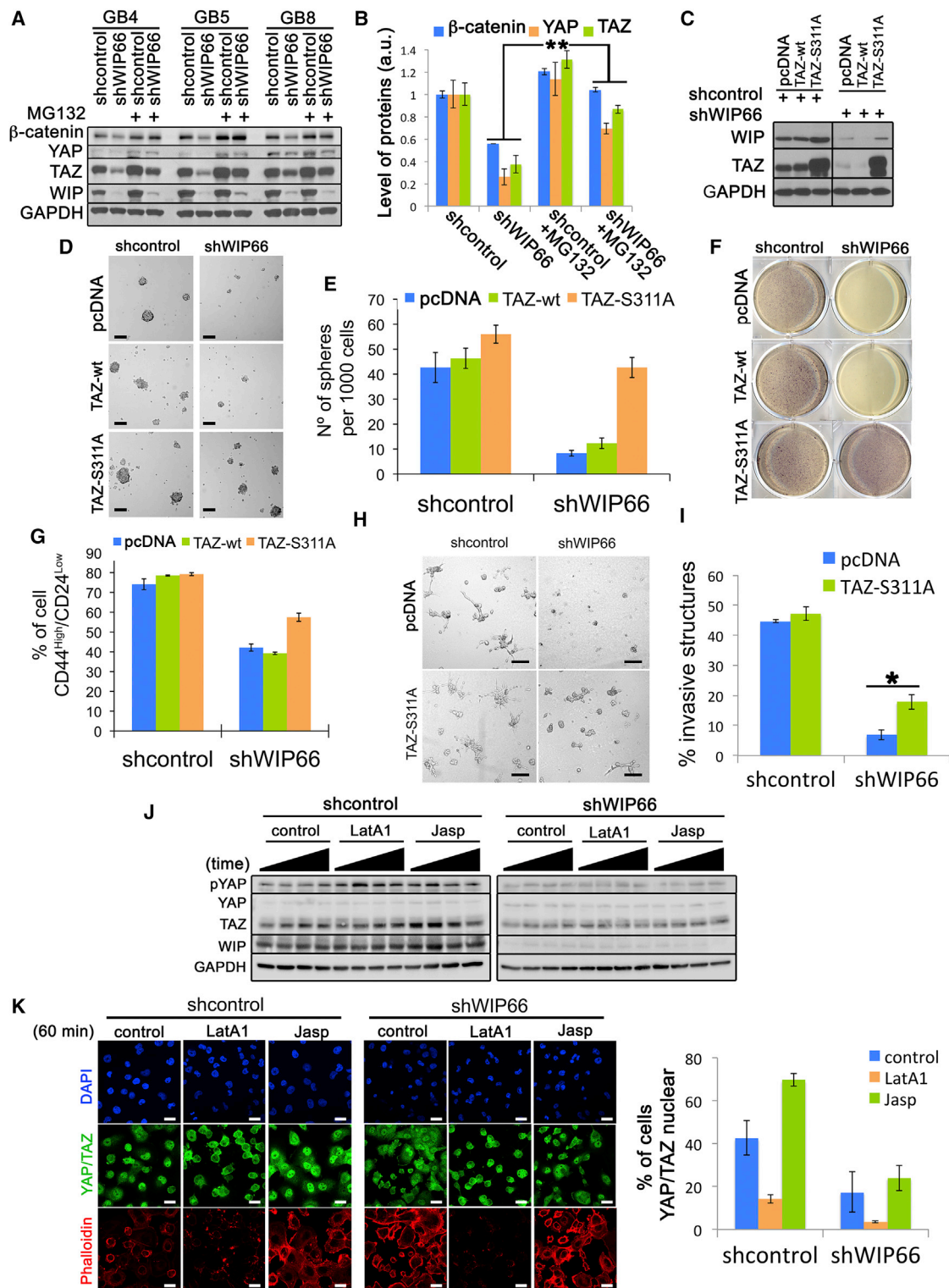


**Figure 5. WIP Regulates TAZ Stability by Controlling Its Degradation by the Proteasome Independently of Actin Dynamics and Hippo Activity** (A and B) Western blot analysis of β-catenin, YAP, TAZ, WIP, and GAPDH expression in GB4, GB5, and GB8 cells knocked down for WIP or control, alone or with proteasome inhibitor (MG132, 10 μM) (A); quantification of GB5 data is shown in (B). (C–I) MDA-MB-231 cells infected with lentivirus shcontrol or shWIP66 and transfected with pcDNA, TAZ-WT, or TAZ-S311A (a degradation-insensitive mutant). (C) Western blot analysis of WIP, TAZ, and GAPDH expression.

(legend continued on next page)

(Figures S6K and S6L). These data suggest that this WIP-mediated process is controlled upstream of APC/axin/GSK3 sequestration.

### WIP Stabilization of YAP/TAZ Is Rac/PAK- and Mammalian Diaphanous-Related-Dependent

Our screening experiment showed that Rac, PAK, and formin inhibitors had a clear effect on WIP-induced cell viability (Figure 6A). An in-depth study of GTPase function in our model of YAP/TAZ stabilization by WIP showed that the Rac inhibitor (NSC23766) reversed WIP ability to stabilize YAP/TAZ, which was unaffected by Cdc42 (casin) or RhoA (Y16) inhibitors in astrocytes (Figure S7A) and GB (Figures S7B and S7C). In contrast, WIP knockdown did not destabilize YAP/TAZ in the presence of a constitutively active Rac mutant (RAC-V12) (Figure S7D). In GB, WIP knockdown also reduced the phosphorylation levels of PAK (Figure S7E), a Rac substrate in many processes. All of these results demonstrate a pivotal role for Rac in WIP-mediated cell survival that is consistent with studies showing that Rac is essential for tumor growth (Feng et al., 2011; Man et al., 2014).

We analyzed two other inhibitors identified by our screening, IPA-3 (PAK1-specific) and SMIFH2 (formins). Under stem culture conditions, IPA-3, SMIFH2, or LatA1 greatly reduced WIP-GFP astrocyte growth, with similar results for GB (Figures 7A and 7B; Figures S7F–S7H). Biochemical analysis of extracts from these cells showed that WIP expression initially increased TAZ, which was subsequently reduced by SMIFH2 and more severely by IPA-3 (Figure 7A; Figures S7F–S7H). The results for both inhibitors were similar in MDA-MB-231-purified TICs (Figures S7I and S7J), which verified WIP involvement in TIC maintenance and cancer pathology. Immunofluorescence analysis showed a clear reduction (>50%) in YAP/TAZ-positive nuclei after IPA-3, SMIFH2, or LatA1 treatment (Figures 7C and 7D). These inhibitors also reduced the TEAD- and  $\beta$ -catenin-mediated transcription induced by WIP overexpression (Figures 7E and 7F). Although our previous findings showed that inhibition of actin polymerization did not result in loss of YAP/TAZ stability (Figure 5J), we found that LatA1 treatment impaired YAP/TAZ nuclear transit as well as cell growth (Figures 7A–7D; Figures S7I and S7J). Another actin polymerization inhibitor, cytochalasin, gave similar results (data not shown).

To confirm that the mammalian diaphanous-related formin (mDia) and PAK have a major role in the oncogenic function of WIP, we transduced cells with a lentivirus bearing GFP, mDia2, or an active version of PAK (PAK-constitutively active [PAK-CA]) in cells knocked down for WIP or in controls and analyzed tumor cell number and growth. Cell growth hampered by WIP knockdown was rescued by mDia2 or PAK-CA expres-

sion and more so by combined mDia2/PAK-CA (Figures 7G and 7H). A parallel western blot analysis confirmed that mDia2 or PAK-CA recover TAZ levels reduced by WIP elimination (Figure 7G). To extend these studies to the APC/axin/GSK-3 sequestration model, we cultured MDA-MB-231 cells alone or with IPA-3 or SMIFH2. A proteinase K protection assay showed impaired GSK3 and axin sequestration, and GSK3 did not co-localize with the LysoTracker marker (Figures 7I and 7J). These data strongly suggest that WIP controls TAZ levels by an mDia2- and Rac/PAK-dependent vesicle protection mechanism.

Our findings show an unreported WIP function that coordinates cell processes such as endocytosis, vesicular regulation, proliferation, stemness, and invasiveness, leading to the regulation of YAP/TAZ degradation.

## DISCUSSION

### WIP Is Associated with Tumor Growth and Stem Phenotype

The discovery of stemness in a small cell population within a tumor led to the development of new tumor paradigms that include heterogeneity, asymmetric growth, and the ability to induce new tumors or metastases (Valastyan and Weinberg, 2011). This finding has allowed better understanding of cancer pathology, although the signals that promote establishment of these tumors remain to be addressed. Here we show that WIP regulates the endocytic/endosomal system, inducing sequestration of the  $\beta$ -catenin destruction complex to stabilize YAP/TAZ and  $\beta$ -catenin.

WIP participates in many cellular processes, some of which are relevant in cancer, such as migration and invadopodium formation (García et al., 2014). In yeast, it is also involved in endocytosis and cell growth (Vaduva et al., 1999), although WIP involvement in mammalian cell growth and/or proliferation has not been studied in detail. The full-length structure of WIP is necessary to promote proliferation, stemness, and transformation capacity because the WIP deletion mutants tested (Nck or actin binding sites) do not have the same effect as the full protein, as was also found in other mutants, such as deletion of N-WASP or cortactin binding sites (data not shown). We therefore speculate that WIP acts as a scaffold for various protein complexes that control the endocytic/endosomal system. Our results show that WIP is clearly involved in cell growth and is also directly associated with cancer pathology, as interpreted from the close relationship between WIP expression and basic proliferation markers such as MAPK. It is also one of the few proteins associated with the actin cytoskeleton that have been implicated in tumorigenesis and TIC growth.

(D–F) Representative images of secondary sphere formation (D; scale bars, 50  $\mu$ m), number of secondary spheres (E), and colonies in soft agar (F).

(G) Percentage of CD44<sup>High</sup>/CD24<sup>Low</sup> population as determined by flow cytometry.

(H and I) Representative images of MDA-MB-231 cells grown in 3D Matrigel (H; 6 days; scale bars, 25  $\mu$ m) and their quantification (I).

(J) Western blot analysis of pYAP, YAP/TAZ, WIP, and GAPDH in MDA-MB-231 cells knocked down for WIP or control, alone or with LatA1 (1  $\mu$ M) or jasplakinolide (Jasp, 0.5  $\mu$ M) for increasing times (up to 120 min).

(K) Confocal images of the staining for nuclei (DAPI, blue), YAP/TAZ (green), and F-actin (phalloidin, red) of cells treated for 60 min as in (J) and their quantification. Scale bars, 20  $\mu$ m.

(B, E, G, I, and K) Data are shown as mean  $\pm$  SEM (n = 3).

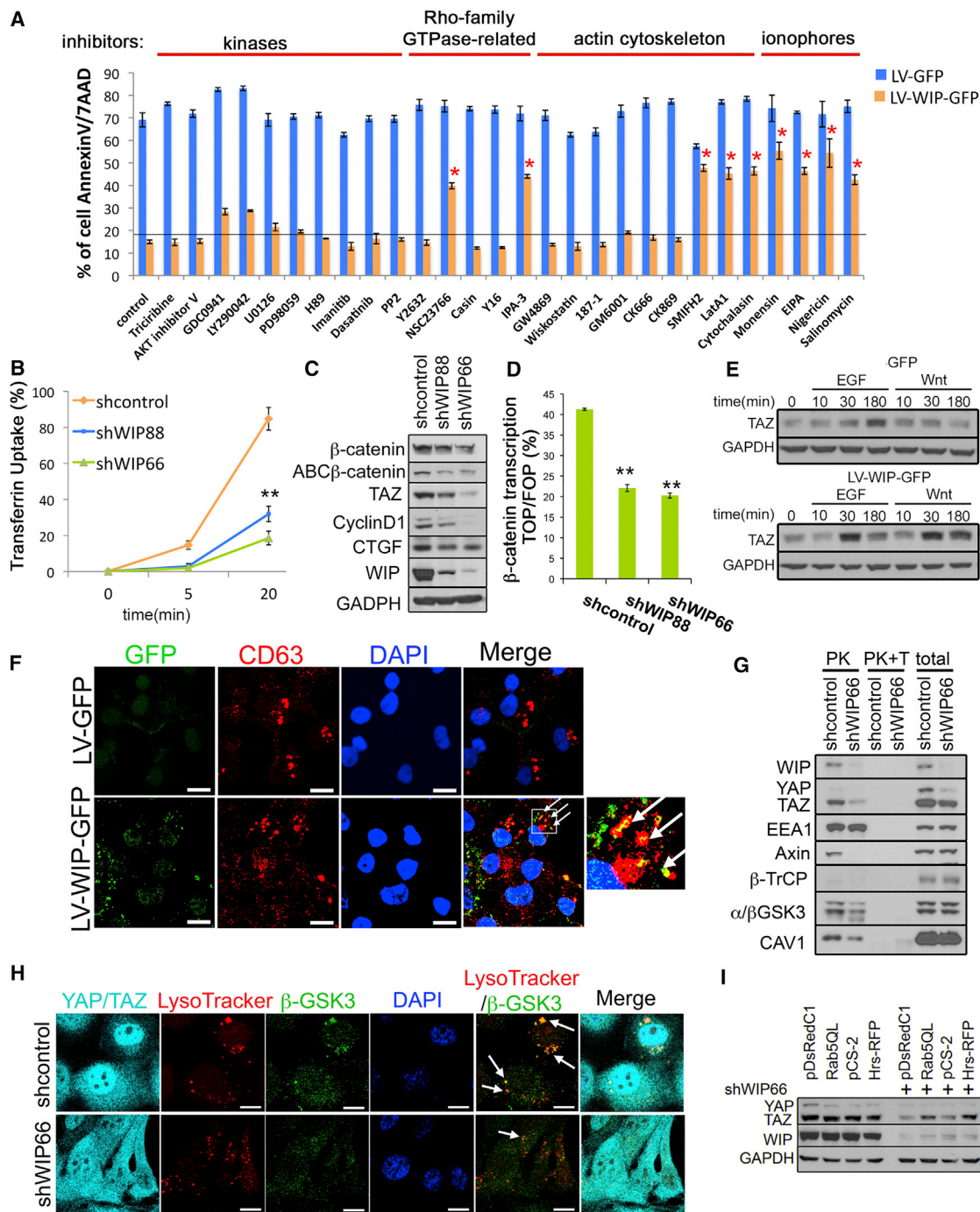


**Figure 6. WIP Is Located in Endosomal Compartments and Requires the APC/Axin/ $\beta$ -GSK3 Destruction Complex to Degrade YAP/TAZ**  
 (A) Screening for synthetic lethal compounds by measuring apoptosis induction (annexin V/7AAD staining) in GFP- or WIP-GFP-overexpressing astrocytes cultured under stem conditions and treated with a panel of inhibitors.  
 (B) Flow cytometry measurement of Alexa 647-transferrin uptake by MDA-MB-231 cells transduced with an shcontrol- or shWIP-encoding lentivirus and cultured under stem conditions.  
 (C) Western blot analysis of  $\beta$ -catenin, ABC- $\beta$ -catenin, TAZ, cyclin D1, CTGF, WIP, and GAPDH in MDA-MB-231 cells transduced as in (B).  
 (D) Quantification of  $\beta$ -catenin-dependent transcription measured by TOP/FOP-GFP in flow cytometry in MDA-MB-231 cells expressing GFP under TOP or FOP sequence control and transduced as in (B).  
 (E) Western blot analysis of TAZ stabilization in GFP-expressing (top) or WIP-GFP-expressing (bottom) astrocytes treated with EGF (100 ng/ml) or Wnt3A (80 ng/ml) at the times indicated.

(legend continued on next page)

### WIP-Mediated YAP/TAZ Stabilization Does Not Involve Actin Cytoskeleton Stability or Activation of the Hippo Pathway

The Hippo pathway and its regulation of YAP/TAZ are found in development, tissue homeostasis, and cancer. This pathway is regulated principally by actin polymerization, which directly affects YAP/TAZ-mediated transcription (Piccolo et al., 2014). WIP can promote the nuclear transit of myocardin-related transcription factor-serum response factor (MRTF-SRF), which is regulated by actin polymerization (Ramesh et al., 2014). Because both YAP/TAZ and MRTF-SRF transcription factors depend on actin polymerization to reach the nucleus, we considered the possibility that WIP regulates YAP/TAZ intracellular distribution.

Our results indicate that WIP elimination induces YAP/TAZ proteolysis through its natural degradation route, the proteasome; a degradation-insensitive TAZ mutant was able to reverse the phenotype caused by WIP knockdown. In the classical Hippo pathway, Hippo-mediated YAP/TAZ regulation mechanisms control the number of phosphorylations that determine YAP/TAZ binding to actin, angiomotin (AMOT), and/or 14.3.3; this prevents YAP/TAZ nuclear transit and/or predisposition to degradation (Piccolo et al., 2014). In many studies, it is nonetheless difficult to discern how much YAP/TAZ transcription control is mediated by its degradation or because of impairment of its nuclear traffic.

YAP/TAZ is activated by mechanotransduction in an actin-dependent fashion, as indicated by the use of actin polymerization inhibitors such as LatA, or low-adhesion surfaces, or inhibitors of Rho, Rho-associated coiled-coil containing protein kinase (ROCK), or myosin, all of which impair nuclear YAP/TAZ transit (Dupont et al., 2011). In the absence of adhesion, YAP/TAZ is regulated by Hippo, which impairs nuclear transit and subsequent transcription (Zhao et al., 2012). Some of these reported data indirectly evaluated YAP/TAZ stability by nuclear transit or transcriptional capacity, while it strictly correlated with actin polymerization; results might be induced by AMOT- or 14.3.3-mediated YAP/TAZ sequestration in the cytosol, which would not necessarily affect complex stability. This might also be the case for actin cytoskeleton regulators such as cofilin, capping protein Z disk (CapZ), or gelsolin (Aragona et al., 2013). Although important in physiological regulation of the Hippo-YAP/TAZ pathway, these mechanisms do not explain the YAP/TAZ increase in various tumor types such as high-grade breast carcinomas (Cordenonsi et al., 2011) or GB (Bhat et al., 2011). In the TIC model, we found that YAP/TAZ nuclear transit is blocked by actin polymerization inhibitors (LatA or cytochalasin); however, the stability of this complex is unimpaired.

Our data show a correlation between high WIP levels and WIP-induced YAP/TAZ stability, which leads to increased transcription, proliferation, stemness, and invasiveness. Because WIP knockdown did not induce an increase in Lats1 (Hippo)-dependent YAP/TAZ phosphorylation, we speculate that WIP removal does not activate the Hippo pathway. WIP thus regulates YAP/TAZ stability via a mechanism in which actin polymerization and the Hippo pathway are secondary effectors. It is tantalizing to consider that actin polymerization has an essential role in YAP/TAZ nuclear transit and/or cytoplasmic retention.

### WIP Regulates the Endocytic/Endosomal System and Thus Induces Destruction Complex Sequestration in MVBS

Although endocytosis was initially only considered a mechanism to limit signal transduction, the endocytic/endosomal pathway was recently shown to have other roles (Dobrowolski and De Robertis, 2011) in generating a second signaling wave that can increase, disable, or extend signals from a receptor activated in the membrane. For  $\beta$ -catenin transcription in the Wnt pathway, the  $\beta$ -catenin degradation complex must be sequestered. Taelman et al. (2010) showed that sequestration of this destruction complex by the MVB system inhibits  $\beta$ -catenin degradation. In the context of Wnt stimulation, the same APC/axin/GSK3 destruction complex is responsible for stabilizing YAP/TAZ transcription factors, whose synergy promotes gain of tumor function (Azzolin et al., 2012, 2014).

In our model, WIP elimination also affects  $\beta$ -catenin stability and transcription, which parallel the loss of YAP/TAZ stability. Our findings for  $\beta$ -catenin suggested that the formation and/or function of the destruction complex are affected by lack of WIP. In axin1 immunoprecipitation assays, formation of the APC/axin/GSK3 destruction complex was unaffected by WIP knockdown (data not shown). After WIP elimination,  $\beta$ -catenin and APC mutants controlled the destruction complex by reversing the effect of YAP/TAZ degradation.

We propose that much of YAP/TAZ stabilization is linked to  $\beta$ -catenin regulation in situations of high WIP levels, as was shown for Wnt. This raises some questions as to whether WIP stabilizes tumor cells with high levels of only YAP/TAZ or  $\beta$ -catenin transcription factors.

Using a model of WIP-overexpressing human primary astrocytes, we evaluated a panel of specific inhibitors that impaired the WIP effect on cell survival. A group of these compounds shows WIP involvement in endocytosis; these include the  $\text{Na}^+/\text{H}^+$  exchanger inhibitor EIPA, which blocks receptor endocytosis, and the  $\text{Na}^+$  ionophore monensin, which affects the endocytosis/endosomal system. This finding was

(F) Confocal images of MDA-MB-231 cells transduced with GFP- or WIP-GFP-encoding lentiviruses, treated with saponin (5 min), and immunostained for CD63. Scale bars, 10  $\mu\text{m}$ . Inset: magnification of the boxed area and arrows; codistribution of WIP and CD63.

(G) Proteinase K protection assay of MDA-MB-231 cells knocked down for WIP or control and analyzed by western blot for WIP, YAP/TAZ, EEA1, axin,  $\beta$ TrCP,  $\alpha/\beta$ -GSK3, and caveolin.

(H) Representative confocal images of MDA-MB-231 cells knocked down for WIP or control and treated with saponin (5 min), showing anti-YAP/TAZ (cyan), LysoTracker (red), anti- $\beta$ GSK3 (green), and DAPI (blue). Scale bars, 10  $\mu\text{m}$ .

(I) Western blot analysis of YAP/TAZ and WIP in cells knocked down for WIP and transfected with Rab5QL (active) or Hrs-red fluorescent protein (RFP) or their respective control plasmids, pDsRedC1 and pCS2.

(A, B, and D) Data are shown as mean  $\pm$  SEM ( $n = 3$ ).

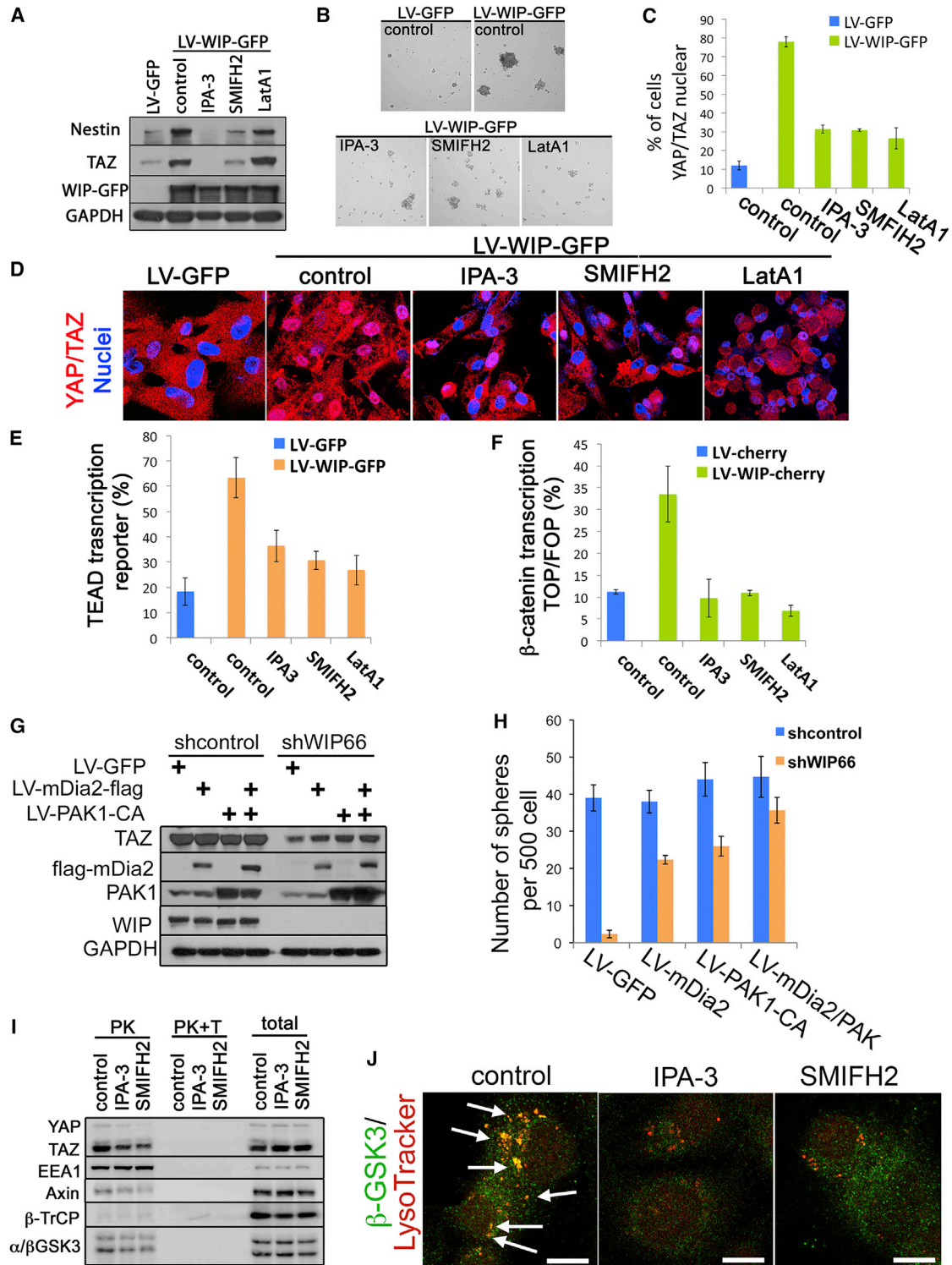


**Figure 7. WIP Stabilizes YAP/TAZ through PAK and mDia**

(A–F) Analysis of astrocytes expressing GFP or expressing WIP-GFP with vehicle (control) or inhibitors of PAK (IPA-3, 10  $\mu$ M), formins (SMIFH2, 30  $\mu$ M), or actin polymerization (LatA1, 1  $\mu$ M).

(A) Western blot analysis of nestin, TAZ, WIP-GFP, and GAPDH.

(B) Representative images of sphere growth.

(C and D) Quantification of astrocytes showing nuclear YAP/TAZ localization (C) and confocal images (D).

(legend continued on next page)

specifically corroborated by measuring transferrin receptor internalization and validated by Wnt3a ligand induction of YAP/TAZ stabilization. WIP co-distributed with CD63, found in intraluminal vesicles of MVBs; we also observed that WIP elimination alters endosomal function and vesicular acidification. These findings permit speculation that sequestration of the APC/axin/GSK3 complex in the MVBs is impaired by the WIP effect on the endosomal system; this is due to YAP/TAZ destabilization generated by WIP knockdown, which can be rescued by overexpression of Rab5QL or Hrs, specific regulators of MVB sequestration.

We show that the K<sup>+</sup> ionophores nigericin and salinomycin (which are specifically toxic for breast TICs; Gupta et al., 2009), monensin, and EIPA destabilize YAP/TAZ and, in parallel, impair GB TIC growth. Based on these data, these ionophores and the Na<sup>+</sup>/H<sup>+</sup> exchanger inhibitor appear to have a common effect on the endocytic/endosomal system by impairing APC/axin/GSK3 complex sequestration and facilitating YAP/TAZ and  $\beta$ -catenin degradation, thus inducing specific TIC cytotoxicity.

PI3K, Rac, and PAK were recently implicated in a newly reported clathrin-independent system responsible for fast endophilin-mediated endocytosis (FEME) of receptors (Boucrot et al., 2015). In addition, formins such as mDia assist membrane receptor transit to caveola vesicles (Echarri et al., 2012). We propose that these proteins, Rac, PAK, and formin, be included in the group of endocytic/endosomal system regulators that WIP needs to coordinate vesicular systems, allow efficient sequestration of the APC/axin/GSK3 destruction complex, and promote YAP/TAZ and  $\beta$ -catenin stability. The PI3K-Rac-Rab5 system is necessary for endosomal-lysosomal system maturation and for MVB formation, and we found that Rac-V12 or PAK-CA/mDia2 overexpression rescues the phenotype generated by lack of WIP.

All of these data strongly support the hypothesis that WIP exerts powerful control on this segment of the Wnt pathway to regulate YAP/TAZ and  $\beta$ -catenin stability through MVB dynamics.

In summary, our results show that WIP drives a mechanism that stimulates cells by rendering growth factor pathways more efficient, enhancing the signaling from endocytosis of membrane receptors to MVBs to increase their effect, and promoting YAP/TAZ and  $\beta$ -catenin stability. These high YAP/TAZ levels, potentiated by increased WIP levels, can intensify their transcription factor capacity, which allows cells to coordinate key processes in cancer progression, such as proliferation, stemness, and invasiveness. Based on a multistep tumorigenic model, we speculate

that inhibitors of the WIP pro-tumor function could have effective therapeutic applications.

## EXPERIMENTAL PROCEDURES

### Survival Analyses

WIP gene expression and survival data from human GB tumors corresponding to The Cancer Genome Atlas (TCGA) and Freije datasets were downloaded, respectively, from the cBioPortal (<http://www.cbioportal.org/>) and GEO databases (<http://www.ncbi.nlm.nih.gov/gds>) (GEO: GSE4412). Kaplan-Meier survival curves were done following patient stratification using WIP expression values as described in the [Supplemental Experimental Procedures](#).

### Cell Culture, Reagents, and Plasmids

GB and cell lines were cultured, transfected, transduced, and/or infected as described previously (Gargini et al., 2015). For complete details on plasmids, reagents, or specific procedures, see the [Supplemental Experimental Procedures](#).

### Lentiviral and Retroviral Vector Production and Infection

Lentiviral vectors were produced using reagents and protocols as reported previously (Gargini et al., 2015). See the [Supplemental Experimental Procedures](#) for specific details.

### WIP Expression in Human GB Subtypes

Classification into classical, mesenchymal, neural, and proneural subtypes was retrieved from the TCGA GB dataset (<https://www.ncbi.nlm.nih.gov/pubmed/24120142>) together with WIP expression values. Differences in WIP expression between mesenchymal and other groups was calculated using Student's t test.

### GB Collection and Intracranial Tumor Assay

Human GBs were kindly supplied by Dr. Izquierdo (Hospital Ramón y Cajal) and derived from brain surgery biopsies of patients with the approval of the hospital ethical committees and that of the Centro de Biología Molecular Severo Ochoa (CBMSO)-Universidad Autónoma de Madrid (UAM) (SAF 2009-07259, issue date February 26, 2009).

All mouse experiments were performed according to national and European Union guidelines basically as described previously (Anido et al., 2010). The protocol was approved by the Committee on the Ethics of Animal Experiments of the UAM (SAF2012-39148-C03-01) and by the CBMSO institutional Biosafety Committee. See the [Supplemental Experimental Procedures](#) for further details.

### Western Blots, Immunofluorescence Analysis, Flow Cytometry Analysis, Cell Sorting, and Antibodies

Western blots, indirect immunofluorescence (monolayer, 2D, or 3D), flow cytometry analysis, and cell sorting were performed as described previously (Gargini et al., 2015). For complete details on immunostaining and antibodies, see the [Supplemental Experimental Procedures](#).

### Quantitative Real-Time PCR Assays

Total RNA was prepared with the RNeasy kit (QIAGEN). See the [Supplemental Experimental Procedures](#) for specific details and primers.

(E and F) Quantification by flow cytometry of TEAD-dependent (E) or  $\beta$ -catenin-dependent (F) transcription.

(G and H) MDA-MB-231 cells knocked down for WIP or control and transduced with a GFP-, mDia2-, PAK1-CA-, or mDia2/PAK1-CA-encoding lentivirus and cultured under stem conditions.

(G) Western blot analysis of TAZ, FLAG-mDia2, PAK1, WIP, and GAPDH.

(H) Quantification of sphere number.

(I) Proteinase K protection assay of MDA-MB-231 cells treated with vehicle (DMSO, control), IPA-3 (10  $\mu$ M), or SMIFH2 (30  $\mu$ M) and western blot analysis of YAP/TAZ, EEA1, axin,  $\beta$ -TrCP, and  $\alpha$ / $\beta$ -GSK3.

(J) Representative confocal images of MDA-MB-231 cells incubated with vehicle (DMSO, control), IPA-3, or SMIFH2 as in (I), stained (5 min) with LysoTracker (red), permeabilized with saponin, and fixed with paraformaldehyde (PFA). Fixed cells were immunostained with anti- $\beta$ GSK3. Arrows indicate LysoTracker and anti- $\beta$ GSK3 codistribution. Scale bars, 10  $\mu$ m.

(C, E, F, and H) Data are shown as mean  $\pm$  SEM (n  $\geq$  3).

### Statistical Analysis

Quantitative data, represented as mean  $\pm$  SEM, were compared between groups using two-tailed Student's *t* test. Differences are presented with statistical significance or *p* value (\**p* < 0.05; \*\**p* < 0.01; NS, not significant). For correlation analysis between each protein, expression data were tested by Pearson's correlation coefficient (R2); *p* values are indicated in the figures. For survival analyses, we used the Kaplan-Meier method and log-rank tests.

### SUPPLEMENTAL INFORMATION

Supplemental Information includes Supplemental Experimental Procedures and seven figures and can be found with this article online at <http://dx.doi.org/10.1016/j.celrep.2016.10.064>.

### AUTHOR CONTRIBUTIONS

R.G. and M.E. performed the experiments. R.G. and R.G.E. contributed to the bioinformatics analysis. R.G., M.E., E.G., F.W., and I.M.A. designed the experiments, analyzed the data, wrote the manuscript, and provided editorial suggestions and criticism.

### ACKNOWLEDGMENTS

We thank Catherine Mark for editorial assistance. R.G. received a J. de la Cierva fellowship from the Spanish Ministry of Science and Innovation (MICINN). This work was supported by grants from the MINECO (SAF2013-45937-R to I.M.A.) and MINECO/FEDER (SAF2015-70368-R to I.M.A. and F.W.), the European Union (EU-FP7-2009-CT222887 to F.W.), the Instituto de Salud Carlos III Centro de Investigación Biomédica en Red (CIBERNED to F.W.) and by a grant from ISCIII-RETIC (RD12/0036/0009 to R.G.E.).

Received: April 19, 2016

Revised: September 12, 2016

Accepted: October 18, 2016

Published: November 15, 2016

### REFERENCES

- Anido, J., Sáez-Bordería, A., González-Juncà, A., Rodón, L., Folch, G., Carmona, M.A., Prieto-Sánchez, R.M., Barba, I., Elena Martínez-Sáez, E., Prudkin, L., et al. (2010). TGF- $\beta$  receptor inhibitors target the CD44<sup>high</sup>/Id1<sup>high</sup> glioma-initiating cell population in human glioblastoma. *Cancer Cell* **18**, 655–668.
- Antón, I.M., Jones, G.E., Wandosell, F., Geha, R., and Ramesh, N. (2007). WASP-interacting protein (WIP): working in polymerisation and much more. *Trends Cell Biol.* **17**, 555–562.
- Aragona, M., Panciera, T., Manfrin, A., Giullitti, S., Michielin, F., Elvassore, N., Dupont, S., and Piccolo, S. (2013). A mechanical checkpoint controls multicellular growth through YAP/TAZ regulation by actin-processing factors. *Cell* **154**, 1047–1059.
- Azzolin, L., Zanconato, F., Bresolin, S., Forcato, M., Basso, G., Biciato, S., Cordenonsi, M., and Piccolo, S. (2012). Role of TAZ as mediator of Wnt signaling. *Cell* **151**, 1443–1456.
- Azzolin, L., Panciera, T., Soligo, S., Enzo, E., Biciato, S., Dupont, S., Bresolin, S., Frasson, C., Basso, G., Guzzardo, V., et al. (2014). YAP/TAZ incorporation in the  $\beta$ -catenin destruction complex orchestrates the Wnt response. *Cell* **158**, 157–170.
- Bhat, K.P., Salazar, K.L., Balasubramanian, V., Wani, K., Heathcock, L., Hollingsworth, F., James, J.D., Gumin, J., Diefes, K.L., Kim, S.H., et al. (2011). The transcriptional coactivator TAZ regulates mesenchymal differentiation in malignant glioma. *Genes Dev.* **25**, 2594–2609.
- Boucrot, E., Ferreira, A.P., Almeida-Souza, L., Debar, S., Vallis, Y., Howard, G., Bertot, L., Sauvonnnet, N., and McMahon, H.T. (2015). Endophilin marks and controls a clathrin-independent endocytic pathway. *Nature* **517**, 460–465.
- Cordenonsi, M., Zanconato, F., Azzolin, L., Forcato, M., Rosato, A., Frasson, C., Inui, M., Montagner, M., Parenti, A.R., Poletti, A., et al. (2011). The Hippo transducer TAZ confers cancer stem cell-related traits on breast cancer cells. *Cell* **147**, 759–772.
- Cottini, F., Hideshima, T., Xu, C., Sattler, M., Dori, M., Agnelli, L., ten Hacken, E., Bertilaccio, M.T., Antonini, E., Neri, A., et al. (2014). Rescue of Hippo coactivator YAP1 triggers DNA damage-induced apoptosis in hematological cancers. *Nat. Med.* **20**, 599–606.
- Dobrowolski, R., and De Robertis, E.M. (2011). Endocytic control of growth factor signalling: multivesicular bodies as signalling organelles. *Nat. Rev. Mol. Cell Biol.* **13**, 53–60.
- Dupont, S., Morsut, L., Aragona, M., Enzo, E., Giullitti, S., Cordenonsi, M., Zanconato, F., Le Digabel, J., Forcato, M., Biciato, S., et al. (2011). Role of YAP/TAZ in mechanotransduction. *Nature* **474**, 179–183.
- Echarri, A., Muriel, O., Pavón, D.M., Azegrouz, H., Escolar, F., Terrón, M.C., Sanchez-Cabo, F., Martínez, F., Montoya, M.C., Llorca, O., and Del Pozo, M.A. (2012). Caveolar domain organization and trafficking is regulated by Abl kinases and mDia1. *J. Cell Sci.* **125**, 3097–3113.
- Feng, H., Hu, B., Liu, K.W., Li, Y., Lu, X., Cheng, T., Yiin, J.J., Lu, S., Keezer, S., Fenton, T., et al. (2011). Activation of Rac1 by Src-dependent phosphorylation of Dock180(Y1811) mediates PDGFR $\alpha$ -stimulated glioma tumorigenesis in mice and humans. *J. Clin. Invest.* **121**, 4670–4684.
- Feng, X., Degese, M.S., Iglesias-Bartolome, R., Vaque, J.P., Molinolo, A.A., Rodrigues, M., Zaidi, M.R., Ksander, B.R., Merlino, G., Sodhi, A., et al. (2014). Hippo-independent activation of YAP by the GNAQ uveal melanoma oncogene through a trio-regulated rho GTPase signaling circuitry. *Cancer Cell* **25**, 831–845.
- García, E., Jones, G.E., Machesky, L.M., and Antón, I.M. (2012). WIP: WASP-interacting proteins at invadopodia and podosomes. *Eur. J. Cell Biol.* **91**, 869–877.
- García, E., Machesky, L.M., Jones, G.E., and Antón, I.M. (2014). WIP is necessary for matrix invasion by breast cancer cells. *Eur. J. Cell Biol.* **93**, 413–423.
- Gargini, R., Cerliani, J.P., Escoll, M., Antón, I.M., and Wandosell, F. (2015). Cancer stem cell-like phenotype and survival are coordinately regulated by Akt/FoxO/Bim pathway. *Stem Cells* **33**, 646–660.
- Gupta, P.B., Onder, T.T., Jiang, G., Tao, K., Kuperwasser, C., Weinberg, R.A., and Lander, E.S. (2009). Identification of selective inhibitors of cancer stem cells by high-throughput screening. *Cell* **138**, 645–659.
- Hanahan, D., and Weinberg, R.A. (2011). Hallmarks of cancer: the next generation. *Cell* **144**, 646–674.
- Hao, Y., Chun, A., Cheung, K., Rashidi, B., and Yang, X. (2008). Tumor suppressor LATS1 is a negative regulator of oncogene YAP. *J. Biol. Chem.* **283**, 5496–5509.
- Joffre, C., Barrow, R., Ménard, L., Calleja, V., Hart, I.R., and Kermorgant, S. (2011). A direct role for Met endocytosis in tumorigenesis. *Nat. Cell Biol.* **13**, 827–837.
- Liu, C.Y., Zha, Z.Y., Zhou, X., Zhang, H., Huang, W., Zhao, D., Li, T., Chan, S.W., Lim, C.J., Hong, W., et al. (2010). The hippo tumor pathway promotes TAZ degradation by phosphorylating a phosphodegron and recruiting the SCFbeta-TrCP E3 ligase. *J. Biol. Chem.* **285**, 37159–37169.
- Man, J., Shoemake, J., Zhou, W., Fang, X., Wu, Q., Rizzo, A., Prayson, R., Bao, S., Rich, J.N., and Yu, J.S. (2014). Sema3C promotes the survival and tumorigenicity of glioma stem cells through Rac1 activation. *Cell Rep.* **9**, 1812–1826.
- Moroishi, T., Hansen, C.G., and Guan, K.L. (2015). The emerging roles of YAP and TAZ in cancer. *Nat. Rev. Cancer* **15**, 73–79.
- Muller, P.A., Caswell, P.T., Doyle, B., Iwanicki, M.P., Tan, E.H., Karim, S., Lukashchuk, N., Gillespie, D.A., Ludwig, R.L., Gosselin, P., et al. (2009). Mutant p53 drives invasion by promoting integrin recycling. *Cell* **139**, 1327–1341.
- Piccolo, S., Dupont, S., and Cordenonsi, M. (2014). The biology of YAP/TAZ: hippo signaling and beyond. *Physiol. Rev.* **94**, 1287–1312.
- Ramesh, N., Massaad, M.J., Kumar, L., Koduru, S., Sasahara, Y., Anton, I., Bhasin, M., Libermann, T., and Geha, R. (2014). Binding of the WASP/N-WASP-interacting protein WIP to actin regulates focal adhesion assembly and adhesion. *Mol. Cell Biol.* **34**, 2600–2610.



- Schafer, D.A. (2002). Coupling actin dynamics and membrane dynamics during endocytosis. *Curr. Opin. Cell Biol.* *14*, 76–81.
- Shibue, T., Brooks, M.W., and Weinberg, R.A. (2013). An integrin-linked machinery of cytoskeletal regulation that enables experimental tumor initiation and metastatic colonization. *Cancer Cell* *24*, 481–498.
- Stevenson, R.P., Veltman, D., and Machesky, L.M. (2012). Actin-bundling proteins in cancer progression at a glance. *J. Cell Sci.* *125*, 1073–1079.
- Taelman, V.F., Dobrowolski, R., Plouhinec, J.L., Fuentealba, L.C., Vorwald, P.P., Gumper, I., Sabatini, D.D., and De Robertis, E.M. (2010). Wnt signaling requires sequestration of glycogen synthase kinase 3 inside multivesicular endosomes. *Cell* *143*, 1136–1148.
- Vaduva, G., Martinez-Quiles, N., Anton, I.M., Martin, N.C., Geha, R.S., Hopper, A.K., and Ramesh, N. (1999). The human WASP-interacting protein, WIP, activates the cell polarity pathway in yeast. *J. Biol. Chem.* *274*, 17103–17108.
- Valastyan, S., and Weinberg, R.A. (2011). Tumor metastasis: molecular insights and evolving paradigms. *Cell* *147*, 275–292.
- Vinyoles, M., Del Valle-Pérez, B., Curto, J., Viñas-Castells, R., Alba-Castellón, L., García de Herreros, A., and Duñach, M. (2014). Multivesicular GSK3 sequestration upon Wnt signaling is controlled by p120-catenin/cadherin interaction with LRP5/6. *Mol. Cell* *53*, 444–457.
- Zhao, B., Li, L., Wang, L., Wang, C.Y., Yu, J., and Guan, K.L. (2012). Cell detachment activates the Hippo pathway via cytoskeleton reorganization to induce anoikis. *Genes Dev.* *26*, 54–68.